

# On the Observation of Intervalence Charge Transfer Bands in Hydrogen-Bonded Mixed-Valence Complexes

Gabriele Canzi, John C. Goeltz, Jane S. Henderson, Roger E. Park, Chiara Maruggi, and Clifford P. Kubiak\*

Department of Chemistry and Biochemistry, University of California San Diego, 9500 Gilman Dr. MC 0358, La Jolla, California 92093-0358, United States

**S** Supporting Information

**ABSTRACT:** Ruthenium clusters of the type  $[\text{Ru}_3(\mu_3\text{O})(\text{OAc})_6(\text{CO})(\text{L})(\text{nic})]$ , where L = 4-dimethylamino-pyridine (dmap) and nic = isonicotinic acid, form hydrogen-bonded mixed-valence dimers upon a single electron reduction. Electrochemical responses show two overlapping reduction waves, indicating the presence of a thermodynamically stable mixed-valence dimer with considerable electronic coupling across the hydrogen bond. Electronic spectra of the singly reduced hydrogen-bonded mixed-valence dimer reveal two intervalence charge transfer bands in the near-infrared region consistent with a Robin-Day class II system. These bands are assigned as metal-to-metal and metal-to-bridge charge transfer, and their behavior is best described by a semiclassical three state model. Infrared spectroscopy suggests localized behavior indicating electron transfer between the two clusters is slower than  $10^{10} \text{ s}^{-1}$ .

The study of electron transfer (ET) processes through noncovalent interactions is essential in the broader understanding of how long-range electron transfer occurs in biological and artificial supramolecular systems and has been a topic of considerable interest in recent years.<sup>1–8</sup> Of the noncovalent interactions that define the spatial arrangement of these types of structures, hydrogen bonds are ubiquitous, and although very few examples exist, hydrogen bonded mixed-valence complexes serve as important models for biological ET.<sup>1,3,7–10</sup>

Using isonicotinic acid as an ancillary ligand, complex **1** was synthesized according to previous reports (Supporting Information, SI). The carboxylic acid functional group is the basis for the formation of cyclic hydrogen-bonded dimers following a one-electron reduction, as shown in Figure 1. Measurement of electrochemical responses is essential to elucidate the mechanism for the ground-state ET reaction. Cyclic voltammetry in a 0.1 M tetrabutylammonium hexafluorophosphate solution in acetonitrile vs Ag/AgCl reveals two reversible one-electron oxidations at positive potentials (Figure 2, waves A and B) and two overlapping one-electron reductions at negative potentials (Figure 2, waves C and D, respectively) as shown in differential pulse voltammetry results (see Figure S2). The splitting, 285 mV in ACN, between the two oxidative processes, occurring at  $-817$  and  $-532$  mV (Figure 2, waves E and F), is indicative of the presence of a thermodynamically

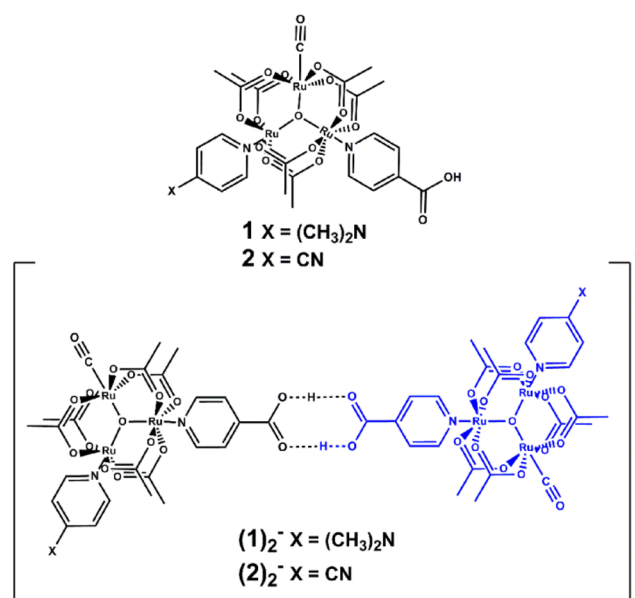


**Figure 1.** Structure of complexes **1** and **2** used in this study and the mixed-valence dimer ion  $(1)_2^{-1}$  and  $(2)_2^{-1}$  formed upon dimerization after a one-electron reduction of **1** and **2**, respectively. A second single-electron reduction yields the doubly reduced dimer,  $(1)_2^{2-}$  and  $(2)_2^{2-}$ .

stable mixed-valence state and moderate electronic communication between the two redox-active  $\text{Ru}_3\text{O}$  clusters due to the formation of a hydrogen-bonded bridge, *vide infra*. Consistent with this interpretation, voltammetric experiments performed in DMSO show a clear disruption of any bridging interaction; only one single-electron reductive wave is observed at reducing potentials.<sup>7</sup>

The comproportionation constant,<sup>11</sup>  $K_c = e^{((nF\Delta E_{1/2})/(RT))}$ , of  $(1)_2^{-}$  is shown to be on the order of  $10^5$  and  $10^3$  for  $(2)_2^{-}$  indicating that the mixed-valence ion is highly stable with respect to the disproportionation reaction.<sup>7</sup> In contrast,  $K_{\text{dim}}$  of unreduced monomer **1** is quite small,  $<0.01$ .<sup>7</sup> Significant electronic coupling in hydrogen-bonded mixed-valence systems has been shown to exist in various systems.<sup>4,12</sup> In fact, hydrogen bonds have been shown to have electronic couplings comparable with covalent  $\sigma$  bonds.<sup>4,13</sup> The observed electrochemical behavior of these  $\text{Ru}_3\text{O}$  clusters in solution is best

Received: October 16, 2013

Published: January 17, 2014

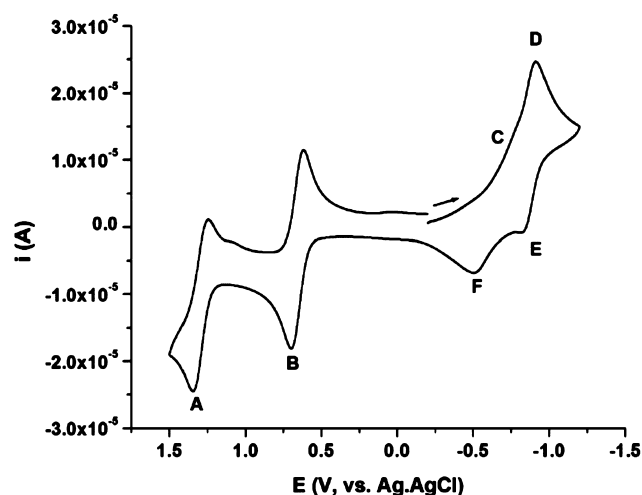


**Figure 2.** Cyclic voltammogram of **1** in acetonitrile at a scan rate of 100 mV/s with a 3 mm glassy carbon working electrode, a Pt counter electrode, and a Ag/AgCl reference. CV measurements were started and ended at 200 mV. At positive potentials two single-electron oxidations are observed (A and B). At negative potentials two overlapping single-electron reductions are apparent (C and D). On the return sweep two distinct reoxidation waves are apparent (E and F), indicative of a ECE mechanism where C is dimerization due to a hydrogen-bonding interaction.

described by an ECE mechanism, where E is attributed to a one-electron reduction and C is dimerization of the complex. The electrochemical splitting of the reoxidation waves (E and F) was found to modulate with solvent choice. As shown in Figure 3, good agreement ( $R^2 = 0.83$ ) was found between the

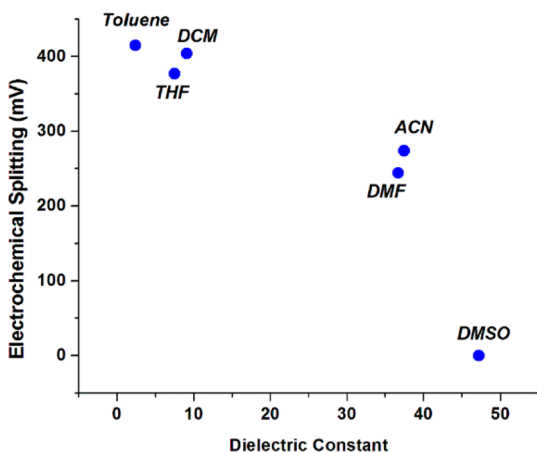


**Figure 3.** Electrochemical splitting of the return waves (1 mM concentration, 100 mV/s scan rate) observed in the electrochemical responses of **1** versus solvent dielectric constants for the solvents used in this study.

electrochemical splitting of E and F with the solvent dielectric constants of the solvents used in this study. This indicates destabilization of mixed valency across hydrogen bonds in higher dielectric media.

FT-IR spectroscopy of neutral (0) monomer **1** shows a  $\nu(\text{CO})$  stretch at  $1945 \text{ cm}^{-1}$ , as expected for  $\text{Ru}_3\text{O}$  carbonyl complexes.<sup>7,14–18</sup> Upon two one-electron reductions, the fully reduced state,  $(\mathbf{1})_2^{2-}$ , exhibits a shift of 50 wavenumbers to  $1895 \text{ cm}^{-1}$ . This shift is consistent with additional electron density on the cluster increasing the  $\pi$  backbonding of the

carbonyl. The mixed-valence state,  $(\mathbf{1})_2^-$ , shows essentially no dynamic coalescence of the  $\nu(\text{CO})$  stretch under the same conditions, signifying localized behavior on the IR time scale with distinct stretches observed at  $1937$  and  $1897 \text{ cm}^{-1}$ , as shown in Figure 4. Localized behavior in FT-IR clearly indicates that the ET process is slower than the vibrational time scale,  $10^{10} \text{ s}^{-1}$ .

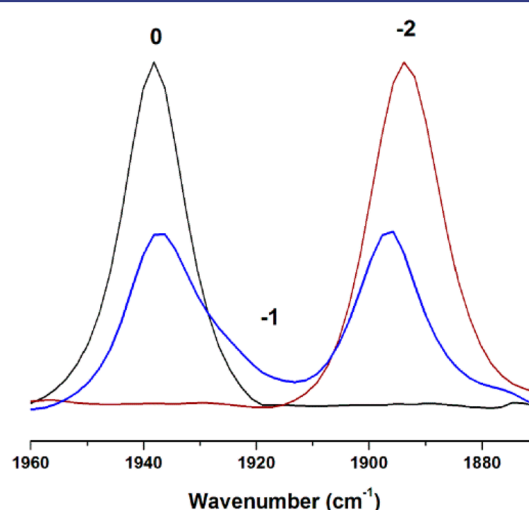


**Figure 4.** FT-IR of the  $\nu(\text{CO})$  in acetonitrile for the neutral (0, black), mixed-valence ( $-1$ , blue), and fully reduced state ( $-2$ , red) of complex **1**. Chemical reductions were performed using bis( $\eta_5$ -pentamethyldienyl)cobalt(II) as the reducing agent. The absence of dynamic coalescence of the  $\nu(\text{CO})$  in the mixed-valence state is evidence of localized behavior on the IR time scale.

The electronic absorption spectra of **1** in acetonitrile show two distinct absorptions in the visible region, analogous to previously reported  $\text{Ru}_3\text{O}$  monomers.<sup>7,14,19,20</sup> The higher energy absorption ( $\lambda_{\text{max}} 399 \text{ nm}$ ,  $\nu_{\text{max}} 25707 \text{ cm}^{-1}$ ,  $\epsilon_{\text{max}} 7260$ ) is assigned as a metal-to-ligand charge transfer (MLCT) and the lower energy absorption ( $\lambda_{\text{max}} 596 \text{ nm}$ ,  $\nu_{\text{max}} 17065 \text{ cm}^{-1}$ ,  $\epsilon_{\text{max}} 5860$ ) is assigned as intracuster charge transfer (ICCT), consistent with literature precedent<sup>14</sup> (see Table 1). Upon a

**Table 1.**  $\lambda_{\text{max}}^a$ ,  $\nu_{\text{max}}^b$ , and  $\epsilon_{\text{max}}$  for MBCT and MMCT for Complexes  $\mathbf{1}_2^-$  and  $\mathbf{2}_2^-$  in Acetonitrile

complex		$\lambda_{\text{max}}$	$\nu_{\text{max}}$	$\epsilon_{\text{max}}$
$\mathbf{1}_2^-$	MBCT	964	10373	3572
	MMCT	1172	8525	2631
$\mathbf{2}_2^-$	MBCT	932	10730	4388
	MMCT	1197	8354	1606

<sup>a</sup>Wavelengths in nm. <sup>b</sup>Energies in wavenumbers.

single one-electron reduction, a concomitant shift and intensification of the ICCT band coupled with a weakening of the MLCT band is apparent. In addition, new bands appear in the near-infrared (NIR) region, diagnostic of two distinct intervalence charge transfer (IVCT) transitions and not one band as expected by the normal two-state Marcus–Hush description of the symmetric mixed-valence complex (Figure 5).<sup>21,22</sup> IVCT bands similar to those observed in the electronic spectra of  $(\mathbf{1})_2^-$  have also been observed in multiple hydrogen-bonded systems by Kaifer, where ferrocene centers showed

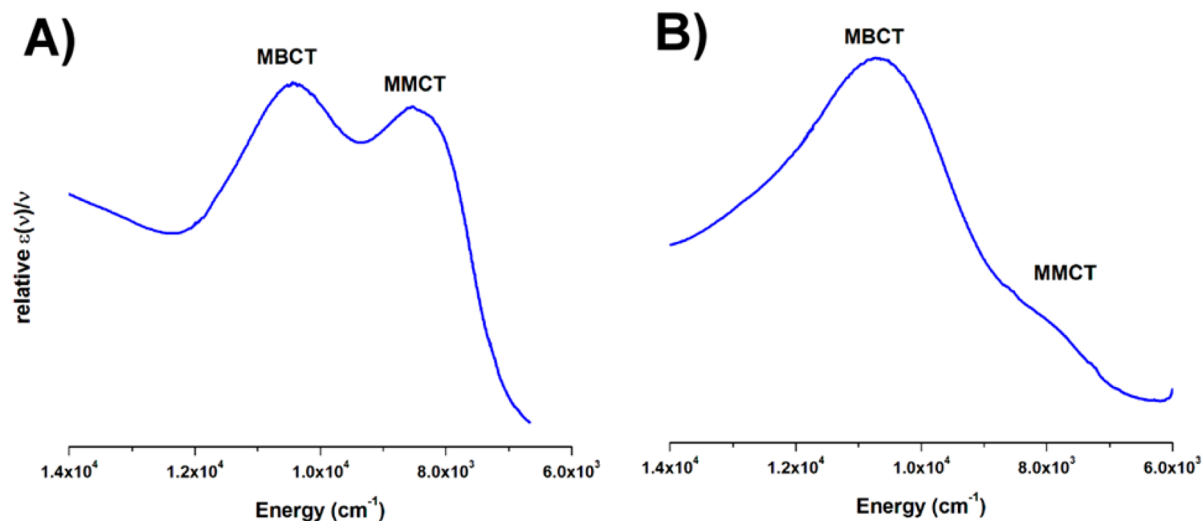


**Figure 5.** NIR region of the electronic absorption spectra of **1** and **2** showing two distinct IVCT bands at 298 K in acetonitrile with an optical pathlength of 0.5 mm using bis( $\eta^5$ -pentamethylcyclopentadienyl)cobalt(II) as a reducing agent. The low-energy band is assigned as a MMCT and the high-energy band as MBCT. Differences in MMCT are attributed to the magnitude of metal-to-bridge coupling due to ancillary ligand substitution.

surprisingly large electronic couplings across large separations between donor and acceptor.<sup>12</sup>

Previous work by our laboratory showed that the appearance and behavior of two IVCT bands in the NIR region of the electronic spectra of pyrazine bridged Ru<sub>3</sub>O dimers was best described by the application of a semiclassical three-state model.<sup>20</sup> The Brunschwig, Creutz, and Sutin (BCS) three-state model uses the basis of a two-state system and adds an additional element for the bridge.<sup>23</sup> The BCS model is parametrized in terms of donor–acceptor coupling, ( $H_{ac}$ ), donor bridge couplings, ( $H_{ab}$ ,  $H_{bc}$ ), and the energy separation between the donor and the bridge state, ( $\Delta G_{ab}$ ). Consistent with the BCS model, the higher energy IVCT band is best described as metal-to-bridge charge transfer (MBCT) since the bridge state is expected to be higher in energy than the metal states.<sup>20,23</sup> The remaining lower energy band can then be assigned as metal-to-metal charge transfer (MMCT).<sup>20,23</sup> These characteristic bands are absent in the electronic absorption spectra after a one electron reduction in DMSO, a hydrogen-bonding solvent that has been shown to disrupt the dimerization of similar systems (SI).<sup>7</sup>

The presence of two IVCT bands is significant because it highlights the importance of the metal-to-bridge coupling. We have previously shown that in other Ru<sub>3</sub>O systems,<sup>14–17</sup> a close match between the  $\pi^*$  levels of the bridge to the  $d\pi$  of the Ru allows for significant electron spin density to be on the bridge.<sup>17</sup>

We probed the effects on metal-to-metal coupling ( $H_{ac}$ ) by varying the donor ability of these systems by tuning the energetics of the clusters by simple ancillary ligand substitution. As shown in Figure 5, when an electron-withdrawing ancillary ligand such as 4-cyanopyridine ( $pK_a \approx 2$ ) is used, the intensity of the MMCT is weaker in comparison to when an electron-donating ligand, such as 4-dimethylaminopyridine ( $pK_a \approx 9$ ), is used. This highlights the importance of metal-to-bridge ( $H_{ab}$  and  $H_{bc}$ ) couplings. The data clearly show that the magnitude of  $H_{ac}$  in these systems is directly related to the magnitude of  $H_{ab}$  and  $H_{bc}$  and that in systems bridged by a noncovalent interaction, such as a hydrogen bond, meaningful metal-to-metal electronic coupling is only observed when there is a substantial metal-to-bridge interaction.

In a donor ( $M_a$ ), bridge ( $B_b$ ), acceptor ( $M_c$ ) system, 1:



each represented by basis functions:

$$\varphi_a, \varphi_b, \varphi_c \quad (2)$$

In the limit of significant delocalization between the metal centers and the bridging ligand, significant mixing between the metal based and bridging ligand functions can occur:

$$\Psi_a = a\varphi_a + b\varphi_b \quad (3)$$

$$\Psi_c = c\varphi_c + b\varphi_b \quad (4)$$

The direct mixing of metal center and bridging ligand wavefunctions, provides an indirect quantum mechanical mechanism for donor–acceptor ( $M_a$ – $M_c$ ) overlap 5:

$$\int \Psi_a \Psi_c \approx \int b^2 \varphi_b^2 \neq 0 \quad (5)$$

It is this metal–ligand mixing which provides significant electronic coupling between metal centers normally considered too far apart or too weakly directly coupled to give a stable mixed-valence state.

Changes in the IVCT bands of **1** in acetonitrile were monitored as a function of temperature from 300 to 258 K. As the temperature is decreased the MBCT and MMCT band intensities increase, and no major shifts in energies are observed (see SI). The intensification of both the MMCT and MBCT is predicted by the BCS model and is due to an increase in  $H_{ac}$  for a class II system at lower temperatures.<sup>23</sup> Minimal or no changes in the energies of these transitions are expected for a localized electronic ground state where solvent dynamic motions are faster than the ground state electron-transfer rate.<sup>20</sup> These results are analogous to purely Robin-Day class II bipyridine bridged mixed-valence dimers previously studied in our laboratory.<sup>20,24</sup>

The results presented are consistent with significant electronic coupling across a large distance between two distinct clusters linked by noncovalent hydrogen-bonding interaction. These studies show that large electronic couplings and high ET

rates are possible in hydrogen-bond systems where there is electronic alignment between metals and the intervening hydrogen-bond bridge. Future work will seek to understand the effects of using other hydrogen-bonding moieties as well as extending the length of these bridges and their geometric orientation in order to examine the effects of donor–acceptor interactions in these hydrogen-bonded systems.

## ■ ASSOCIATED CONTENT

### 📄 Supporting Information

Synthetic and additional experimental details, variable-temperature electronic spectra and infrared spectroscopy results. This material is available free of charge via the Internet at <http://pubs.acs.org>

## ■ AUTHOR INFORMATION

### Corresponding Author

ckubiak@ucsd.edu

### Notes

The authors declare no competing financial interest.

## ■ ACKNOWLEDGMENTS

The authors thank Dr. Bruce S. Brunschwig, Dr. Kyle Grice, Dr. Starla Glover, Candace Seu, and Jesse Froehlich for insightful conversations about these systems. Dr. Anthony Mrse in the UCSD NMR facility for his assistance. We gratefully acknowledge support from the NSF CHE-1145893.

## ■ REFERENCES

- (1) Tadokoro, M.; Inoue, T.; Tamaki, S.; Fujii, K.; Isogai, K.; Nakazawa, H.; Takeda, S.; Isobe, K.; Koga, N.; Ichimura, A.; Nakasuji, K. *Angew. Chem., Int. Ed.* **2007**, *46*, 5938.
- (2) Meyer, T. J. *Acc. Chem. Res.* **1989**, *22*, 163.
- (3) Bonin, J.; Costentin, C.; Robert, M.; Savéant, J.-M.; Tard, C. *Acc. Chem. Res.* **2011**, *45*, 372.
- (4) Rege, P. J. F. d.; Williams, S. A.; Therien, M. J. *Science* **1995**, *269*, 1409.
- (5) Turro, C.; Chang, C. K.; Leroi, G. E.; Cukier, R. I.; Nocera, D. G. *J. Am. Chem. Soc.* **1992**, *114*, 4013.
- (6) Ward, M. D. *Chem. Soc. Rev.* **1997**, *26*, 365.
- (7) Goeltz, J. C.; Kubiak, C. P. *J. Am. Chem. Soc.* **2010**, *132*, 17390.
- (8) Wilkinson, L. A.; McNeill, L.; Meijer, A. J. H. M.; Patmore, N. J. *J. Am. Chem. Soc.* **2013**.
- (9) Pichlmaier, M.; Winter, R. F.; Zabel, M.; Zális, S. *J. Am. Chem. Soc.* **2009**, *131*, 4892.
- (10) Westlake, B. C.; Brennaman, M. K.; Concepcion, J. J.; Paul, J. J.; Bettis, S. E.; Hampton, S. D.; Miller, S. A.; Lebedeva, N. V.; Forbes, M. D. E.; Moran, A. M.; Meyer, T. J.; Papanikolas, J. M. *Proc. Natl. Acad. Sci. U.S.A.* **2011**, *108*, 8554.
- (11) Richardson, D. E.; Taube, H. *Coord. Chem. Rev.* **1984**, *60*, 107.
- (12) Sun, H.; Steeb, J.; Kaifer, A. E. *J. Am. Chem. Soc.* **2006**, *128*, 2820.
- (13) Jakob, M.; Berg, A.; Stavitski, E.; Chernick, E. T.; Weiss, E. A.; Wasielewski, M. R.; Levanon, H. *Chem. Phys.* **2006**, *324*, 63.
- (14) Salsman, J. C.; Ronco, S.; Londergan, C. H.; Kubiak, C. P. *Inorg. Chem.* **2006**, *45*, 547.
- (15) Ito, T.; Hamaguchi, T.; Nagino, H.; Yamaguchi, T.; Kido, H.; Zavarine, I. S.; Richmond, T.; Washington, J.; Kubiak, C. P. *J. Am. Chem. Soc.* **1999**, *121*, 4625.
- (16) Ito, T.; Hamaguchi, T.; Nagino, H.; Yamaguchi, T.; Washington, J.; Kubiak, C. P. *Science* **1997**, *277*, 660–3.
- (17) Kubiak, C. P. *Inorg. Chem.* **2013**.
- (18) Walsh, J. L.; Baumann, J. A.; Meyer, T. J. *Inorg. Chem.* **1980**, *19*, 2145.
- (19) Canzi, G.; Kubiak, C. P. *Small* **2011**, *7*, 1967.
- (20) Glover, S. D.; Kubiak, C. P. *J. Am. Chem. Soc.* **2011**, *133*, 8721.

- (21) Hush, N. S. *Prog. Inorg. Chem.* **1967**, *8*, 391.
- (22) Marcus, R. A. *Annu. Rev. Phys. Chem.* **1964**, *15*, 155.
- (23) Brunschwig, B. S.; Creutz, C.; Sutin, N. *Chem. Soc. Rev.* **2002**, *31*, 168.
- (24) Robin, M. B.; Day, P. *Adv. Inorg. Chem. Radiochem.* **1967**, *10*, 247.